Science, Technology and Innovation
ISSN 2544-9125 ▪ 2026; 25 (2): 1-9
doi: 10.55225/sti.723

STI • 2026; 25 (2): 1-9

Tryptophan as a molecular microswitch: Integrating BioLiP statistical insights with MD simulations of 5-HT$_2$ receptors

Karina Pakosz[1] B-G, Paweł Śliwa[1] A,C-E,G

[1]Cracow University of Technology, Faculty of Chemical Engineering and Technology, Warszawska 24 St, 31-155 Cracow, Poland

Original article

Abstract

Tryptophan residues play a critical role in protein-ligand recognition owing to their unique aromatic character, high polarizability, and ability to participate in diverse noncovalent interactions, including π-π stacking, cation-π interactions, hydrogen bonding, and hydrophobic contacts. In this study, a two-stage approach was employed to elucidate the functional significance of tryptophan residues within ligand-binding sites across diverse protein systems. First, a large-scale statistical analysis was performed using a curated dataset of protein-ligand complexes extracted from the BioLiP database. The dataset was analysed with respect to enzymatic classification and Gene Ontology enrichment, revealing a pronounced enrichment of tryptophan residues in the binding sites of hydrolases, oxidoreductases, and transferases, as well as strong associations with metal-ion binding, redox-related functions, and membrane or cytoplasmic localization. Within the G protein-coupled receptor (GPCR) superfamily, rhodopsin-like class A receptors were identified as the most prominently represented group featuring tryptophan-mediated ligand interactions. In the second stage, molecular dynamics simulations were conducted for selected serotonin 5-HT$_2$ receptor subtypes (5-HT$_2$A, 5-HT$_2$B, and 5-HT$_2$C) to provide atomistic insights into the role of the conserved tryptophan W6.48. The simulations reveal a stable spatial relationship between the ligand and W6.48, characterized by distances consistent with aromatic anchoring, supporting its role in maintaining ligand orientation and binding pocket organization. Collectively, these results highlight tryptophan as a key determinant of ligand recognition and stabilization across both enzymatic and receptor-mediated systems.

Keywords

- tryptophan
- protein–ligand interactions
- molecular dynamics

Authors' contributions

A – Preparation of the research project
B – Assembly of data for the research undertaken
C – Conducting of statistical analysis
D – Interpretation of results
E – Manuscript preparation
F – Literature review
G – Revising the manuscript

Corresponding author

Paweł Śliwa
e-mail: pawel.sliwa@pk.edu.pl
Cracow University of Technology
Faculty of Chemical Engineering and Technology
ul. Warszawska 24
31-155 Kraków, Poland

Article info

Article history

- Received: 2026-03-18
- Accepted: 2026-05-11
- Published: 2026-08-17

Publisher

University of Applied Sciences in Tarnow
ul. Mickiewicza 8, 33-100 Tarnow, Poland

Financing

This research did not receive any grants from public, commercial or non-profit organizations.

Conflict of interest

None declared.

Introduction

Tryptophan (TRP, W) is an essential aromatic amino acid that plays a critical role in protein structure, stability, and molecular recognition [1]. The side chain, consisting of a fused benzene and pyrrole indole ring, features an extended π-electron system with high polarizability. This structure enables tryptophan to participate in diverse noncovalent interactions, including π-π stacking, cation-π interactions, CH-π contacts, hydrophobic interactions, and hydrogen bonding via the indole NH group [2,3]. These interactions support the structural integrity and functional specificity of protein-ligand complexes. The distinct electronic properties of the indole ring set tryptophan apart from other aromatic residues, including phenylalanine and tyrosine, and account for its preferential localization in structurally and functionally important regions of proteins, such as enzyme active sites, ligand-binding pockets, protein-protein interfaces, and transmembrane domains of membrane proteins [4,5]. Tryptophan is not abundant in most proteins, but it can have an outsized effect on how proteins interact with other molecules. Studies show that aromatic amino acids, such as tryptophan, tend to cluster at sites on proteins that are key for binding partners, whether those partners are small molecules or other proteins. At the interfaces where antibodies and antigens meet, tryptophan and tyrosine often show up together and help stabilize the complex by forming clusters that use a mix of aromatic, hydrophobic, and cation-π interactions. This careful arrangement reveals how important tryptophan is for recognizing and binding to the right molecules [5,6]. In membrane proteins, tryptophan residues often localize at the lipid-water interface, where they not only stabilize transmembrane segments but also engage in specific aromatic and polar contacts that contribute to structural ordering and functional interactions [7].

G protein-coupled receptors (GPCRs) are a key component of signalling pathways in eukaryotic cells, enabling the precise transmission of signals from the outside to the inside of the cell and regulating numerous physiological processes [8,9]. Tryptophan residues are critical for GPCR function. Highly conserved amino acids, primarily located in transmembrane domains, help maintain receptor structural stability and support effective signal transduction. Specifically, within ligand binding sites, tryptophan residues can interact directly with ligands. This interaction can stabilize ligand-receptor complexes and facilitate conformational changes required for receptor activation. Consequently, these residues may influence ligand affinity and selectivity [10,11]. In class A GPCRs, highly conserved tryptophan residues, particularly at the Ballesteros-Weinstein position 6.48 within the CWxP motif of transmembrane helix 6 (TM6), are essential for receptor conformational dynamics and activation. Structural and mechanistic studies indicate that this tryptophan is closely integrated into the network of microswitches that connect ligand binding to large-scale rearrangements of the helical bundle, such as the outward movement of TM6 during receptor activation. The orientation and interactions of W6.48 are altered upon agonist binding, thereby linking ligand recognition to the conformational changes required for G-protein coupling and downstream signalling. This aromatic residue contributes to ligand affinity, functional selectivity, and signal transduction efficiency across various GPCR systems [12–14]. Tryptophan residues are distributed across class A GPCR structures and play significant roles in ligand recognition, receptor stability, and conformational transitions linked to activation. Structural and computational studies of the β2-adrenergic receptor reveal that aromatic residues within the transmembrane helices form interaction networks that stabilise receptor conformations and mediate responses to ligand binding [11]. As an illustration, structural studies of the CC-chemokine receptor CCR5 in both agonist-bound and inactive forms show that a conserved tryptophan residue in TM6 ($W248^{6.48}$) is a component of a hydrophobic cleft at the base of the orthosteric pocket. This residue undergoes a conformational shift upon ligand binding, linking chemokine recognition to the outward displacement of TM6, which triggers activation of the canonical microswitch network, including the PIF, NPxxY, and DRY motifs [15]. Comparable ligand-induced changes involving conserved tryptophan residues in TM6 have been reported in additional receptors. For instance, in the neuropeptide Y1 receptor (Y1R), rotameric shifts of W6.48 are associated with structural transitions between active and inactive forms [13]. Similarly, in the adenosine A_2A receptor, $W246^{6.48}$ is involved in microswitch networks that promote TM6 movement and subsequent receptor activation [16]. Analogous roles have also been observed in serotonin (5-HT) receptors, where conserved tryptophan residues within TM6 contribute to ligand binding, stabilize receptor conformations, and facilitate the conformational changes required for G-protein coupling and downstream signalling [17]. Collectively, these studies highlight the critical yet context-dependent roles of tryptophan residues in stabilizing GPCR structures, mediating ligand recognition, and facilitating the conformational transitions necessary for receptor activation.

Materials and methods

The study employed a two-stage approach combining large-scale statistical analysis and molecular dynamics (MD) simulations. The dataset for statistical analysis was extracted from the BioLiP database, a semi-manually curated repository of biologically relevant ligand–protein interactions [18] (1). We also used its updated version, BioLiP2, which provides significantly greater coverage of structural data and enables analysis of large macromolecular complexes [19] (2). Proteins were classified according to Enzyme Commission (EC) numbers and Gene Ontology (GO) terms retrieved from the BioLiP and UniProt databases. This classification allowed for the identification of tryptophan residue frequencies within the binding sites of various functional and enzymatic classes. The BioLiP dataset was filtered to include only entries in which tryptophan (W) is present in the binding-site residues. To ensure data quality, small molecules such as water, ions (e.g., Na^+, K^+, Mg^{2+}), and common crystallization agents (e.g., PEG, glycerol) were excluded. Redundancy was addressed by grouping interactions by PDB ID and Ligand ID, retaining only one representative chain per complex.

Starting systems for the MD simulations of the 5-HT_{2A}, 5-HT_{2B}, and 5-HT_{2C} serotonin receptors (in both active and inactive states) were prepared using the Multicomponent Assembler module in CHARMM-GUI [20–22]. The receptors were embedded in a POPC lipid bilayer, and the systems were solvated with TIP3P water molecules containing 0.1 M KCl. The CHARMM36 force field was used to describe the system parameters, while ligand parameters were generated using the CGenFF 5.0. Simulations were performed using NAMD3 for 100 ns per system, maintaining a constant temperature of 298.15 K. This methodology is analogous to established studies of molecular microswitch dynamics in GPCRs, such as the role of the conserved tryptophan rotamer W6.48 [11]. All geometric analyses of aromatic interactions, including centroid-centroid distances and angles between aromatic ring planes, were performed to determine the stability of the ligand-receptor complexes.

Results and discussion

A statistical analysis of protein-ligand complexes from the Protein Data Bank was conducted to determine the frequency and types of interactions involving tryptophan residues. The dataset comprised protein structures from diverse functional classes, including enzymes and non-enzymatic ligand-binding proteins, such as GPCRs. Proteins were categorized according to EC numbers and functional annotations provided by the BioLiP and UniProt databases.

Distribution of enzyme classes and prevalent enzymes

Within the analysed set of enzyme proteins, hydrolases represented the largest group (11,526 structures), followed by oxidoreductases (10,554) and transferases (8,981). The remaining classes comprised lyases (1,282), isomerases (971), ligases (753), and translocases (597) (Figure 1A). This distribution indicates a predominance of enzymes involved in the decomposition of chemical compounds, transfer of chemical groups, and oxidation-reduction reactions. Among specific enzymes, nitric-oxide synthase (NADPH) (EC 1.14.13.39, 1,822 structures), DNA-directed DNA polymerase (EC 2.7.7.7, 1,147), thrombin (EC 3.4.21.5, 676), and RNA-directed DNA polymerase (EC 2.7.7.49, 543) were the most frequent. The 20 most common enzymes are summarized in Figure 1B. The frequent occurrence of these enzymes in the dataset reflects their broad distribution in nature and their significant roles in interactions with the analysed ligands.

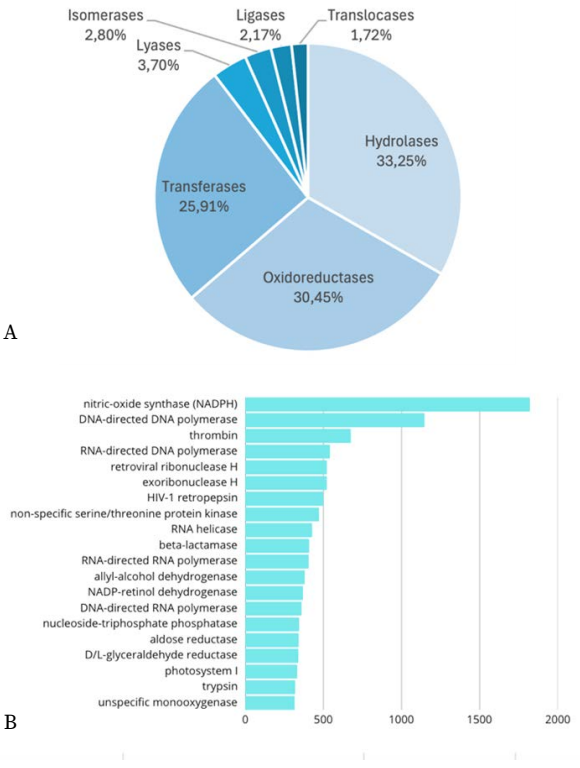

Figure 1. Distribution of enzyme classes and the most frequent enzymes in the dataset. (A) Number of structures per enzyme class; (B) The 20 most frequent enzymes with their respective counts

Gene ontology analysis of tryptophan-containing proteins

To understand the functional and structural contexts of tryptophan residues in proteins, a Gene Ontology (GO) term enrichment analysis was performed. GO terms classify proteins by molecular function, biological process, and cellular localization, enabling the identification of cellular locations and functions where tryptophan residues are particularly abundant.

Tryptophan is most frequently present in proteins associated with metal ion binding (11,451), protein binding (8,796), and oxidoreductase activity (5,817). Within biological processes, proteins containing tryptophan are significantly represented in carbohydrate metabolism (3,310), nitric oxide biosynthesis (2,133), and photosynthesis (1,884). Regarding cellular localization, tryptophan occurs in proteins situated in the cell membrane (membrane, 9,920; plasma membrane, 4,026), cytoplasm (cytoplasm, 9,076; cytosol, 6,798), cell nucleus (nucleus, 3,737; nucleoplasm, 2,076), extracellular structures (extracellular region, 3,156; extracellular space, 2,284), ribosomes (ribosome, 2,114; structural constituent of ribosome, 2,115), and mitochondria (2,659). The findings demonstrate that tryptophan is integral to enzymatic catalysis, ligand binding, and protein structural functions, particularly within ribonucleoprotein complexes and membrane and signalling-related proteins. The presence of tryptophan in such diverse functions and locations underscores its universal importance in protein biology.

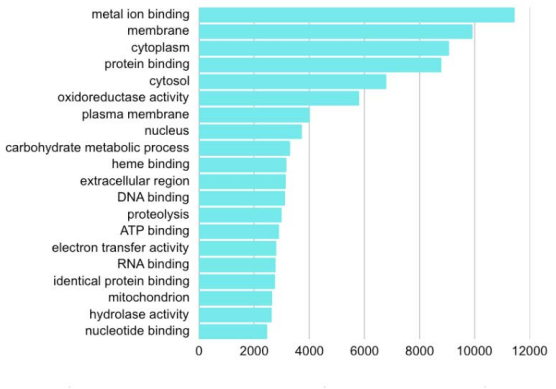

Figure 2. Gene ontology enrichment analysis of proteins containing tryptophan

Distribution and geometric analysis of ligand-tryptophan interactions in class A GPCRs

Records of class A GPCRs containing ligand-tryptophan interactions were grouped according to receptor families, and the number of structures in each group is shown in Figure 3. The highest number of records with ligand-tryptophan interactions was observed for histamine receptors and muscarinic acetylcholine receptors (27 records each). A high representation of interactions involving tryptophan was also found among orphan class A receptors with developing pharmacology (25 records) and opioid receptors (24 records). Other well-represented groups included dopamine receptors (19 records), prostanoid receptors (18 records), and chemokine receptors (17 records). Serotonin (5-hydroxytryptamine) receptors included 9 records containing interactions involving tryptophan. A comparable number of structures was found for adenosine and endothelin receptors (8 records each) and somatostatin receptors (7 records). Other receptor families were represented by a small number of structures, often involving a single case of ligand-tryptophan interaction. The distribution of records across individual families of class A GPCR receptors demonstrates that structures featuring ligand-tryptophan interactions occur in numerous receptor families. However, the number of available records varies among families, reflecting the uneven representation of ligand-bound structures in the database.

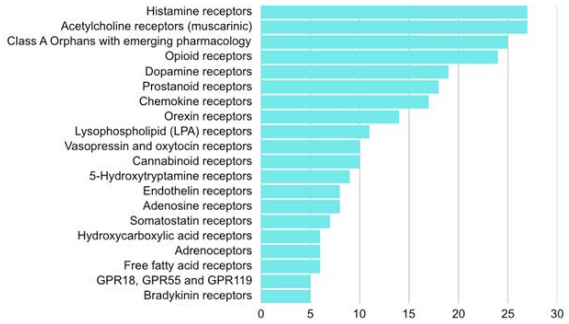

Figure 3. Distribution of ligand-tryptophan interactions across class A GPCR families

An analysis of interactions between ligands and tryptophan residues across 277 unique PDB structures, including 288 cases of TRP-ligand interactions meeting

quality criteria, showed that aromatic interactions exhibit a clearly preferred geometry. Aromatic interactions were classified based on geometric criteria: π–π stacking was defined by a centroid-centroid distance ≤5.5 Å, and an angle between the ligand and TRP ring normal ≤30°. T-shaped interactions were identified when the distance was ≤6.0 Å and the angle was ≥60°. Among the interactions analysed, T-shaped arrangements dominated (58%), while classic π-π stacking was observed much less frequently. The distribution of angles between the planes of aromatic rings was characterized by a median of ~96°, with T-shaped interactions exhibiting significantly larger angles (average ~130°) than other configurations (~42°). The centroid-centroid distances were mainly in the range of 3.9–5.2 Å (median ~4.25 Å), while the minimum atom-atom distances oscillated around 3.5 Å, which is consistent with typical aromatic interaction parameters. These results indicate that tryptophan residues more often stabilize ligands through perpendicular aromatic interactions than through parallel π-π stacking. While this study focuses exclusively on tryptophan, its unique electronic properties—such as the high polarizability of the indole system and its specific capacity for hydrogen bonding via the NH group—distinguish it from other aromatic residues, such as phenylalanine and tyrosine. These features account for its specialized role in ligand anchoring and in stabilizing specific binding geometries. Although a comparative analysis with other aromatic residues represents a promising direction for future research, the current work prioritizes the distinct functional contribution of tryptophan within these complex binding environments.

Tryptophan in the 5-HT_2 receptors binding pockets

5-HT_2 receptors are class A GPCRs that mediate serotonin signalling in both central and peripheral tissues [15,23]. Their ligand-binding pockets are formed by a combination of aromatic and polar residues that determine ligand orientation, binding stability, and receptor activation. Among these residues, tryptophan plays an important role due to its extended indole ring, which enables it to stabilize aromatic and electrostatic interactions with bound ligands. In addition to contributing directly to ligand binding, tryptophan residues influence receptor conformational dynamics by coupling interactions in the binding pocket to conserved activation motifs [24,25]. To examine these effects at the atomic level, molecular dynamics (MD) simulations were performed to analyse ligand-tryptophan interactions and their impact on the conformational behaviour of the 5-HT_2 receptor. To provide a more comprehensive structural perspective, W6.48-ligand distances were analysed across all available crystallographic structures of 5-HT_2 receptors retrieved from GPCRdb [26]. The distance was defined as the centroid-centroid distance between the aromatic ring of the ligand and the indole ring of the W6.48 residue.

Table 1. Analysis of W6.48-ligand distances in all available crystallographic structures of 5-HT_2 receptors from the GPCRdb database

Receptor	PDB ID	State	Ligand Name	Ligand Modality	TRP-Ligand distance [Å]
5-HT_{2A}	8ZMG	Inactive	Pimavanserin	Inverse agonist	6.24
5-HT_{2C}	8ZMF	Inactive	1-[(4-Fluorophenyl)methyl]-1-(5-methyl-5-azaspiro[2.5]octan-8-yl)-3-[[4-(2-methylpropoxy) phenyl]methyl]urea	Inverse agonist	6.94
5-HT_{2A}	8V6U	Active	4-{(3R)-1-[(1R)-1-(pyrimidin-2-yl)ethyl]piperidin-3-yl}phenol	Agonist	8.31
5-HT_{2A}	8UWL	Active	Lisuride	Agonist	8.60
5-HT_{2A}	8JT8	Inactive	1-(4-fluorophenyl)-4-[(7R)-2,5,11-triazatetracyclo[7.6.1.0^2,7.0^12,16]hexadeca-1(15),9,12(16),13-tetraen-5-yl]butan-1-one	Agonist	10.53
5-HT_{2A}	7RAN	Active	3-[(3R)-3-methyl-1,2,3,6-tetrahydropyridin-1-ium-5-yl]-1H-pyrrolo[2,3-b]pyridine	Agonist	9.02
5-HT_{2A}	7WC7	Inactive	Lisuride	Agonist	9.71
5-HT_{2A}	7WC4	Inactive	5-hydroxytryptamine	Agonist	10.75

Receptor	PDB ID	State	Ligand Name	Ligand Modality	TRP-Ligand distance [Å]
5-HT_{2A}	7WC5	Inactive	Psilocin	Agonist	11.17
5-HT_{2A}	7WC8	Inactive	Lumateperone	Agonist	10.43
5-HT_{2A}	7WC9	Inactive	(10~{R},15~{S})-12-[3-(2-methoxyphenyl) propyl]-4-methyl-1,4,12-triazatetracyclo[7.6.1.0^{5,16}.0^{10,15}]hexadeca-5(16),6,8-triene	Agonist	10.31
5-HT_{2A}	7WC6	Inactive	Lysergic acid diethylamide	Agonist	9.48
5-HT_{2A}	7VOD	Inactive	Cariprazine	Partial agonist	9.40
5-HT_{2A}	7VOE	Inactive	Aripiprazole	Partial agonist	6.69
5-HT_{2A}	6WGT	Inactive	Lysergic acid diethylamide	Agonist	9.13
5-HT_{2A}	6WH4	Inactive	Metitepine	Inverse agonist	4.87
5-HT_{2A}	6WHA	Active	4-(2-{[(2-hydroxyphenyl)methyl]amino} ethyl)-2,5-dimethoxybenzonitrile	Agonist	6.50
5-HT_{2A}	6A94	Inactive	Zotepine	Antagonist	4.94
5-HT_{2A}	6A93	Inactive	Risperidone	Antagonist	4.69
5-HT_{2B}	7SRQ	Intermediate	Lysergic acid diethylamide	Agonist	9.83
5-HT_{2B}	7SRS	Active	Lysergic acid diethylamide	Agonist	10.10
5-HT_{2B}	7SRR	Active	Lysergic acid diethylamide	Agonist	10.02
5-HT_{2B}	6DRZ	Intermediate	Methysergide	Antagonist	8.90
5-HT_{2B}	6DRY	Intermediate	Methylergonovine	Agonist	9.04
5-HT_{2B}	6DS0	Intermediate	(8alpha)-N-[(2S)-1-hydroxybutan-2-yl]-1,6-dimethyl-9,10-didehydroergoline-8-carboxamide	Antagonist	8.70
5-HT_{2B}	6DRX	Intermediate	Lisuride	Antagonist	9.48
5-HT_{2B}	5TUD	Active	Ergotamine	Agonist	7.88
5-HT_{2B}	5TVN	Intermediate	Lysergic acid diethylamide	Agonist	9.88
5-HT_{2B}	4NC3	Intermediate	Ergotamine	Agonist	8.15
5-HT_{2B}	4IB4	Intermediate	Ergotamine	Agonist	7.77
5-HT_{2C}	8DPH	Active	Lorcaserin	Agonist	8.47
5-HT_{2C}	8DPG	Active	Psilocin	Agonist	10.61
5-HT_{2C}	8DPF	Active	Lorcaserin	Agonist	8.66
5-HT_{2C}	8DPI	Active	Lorcaserin	Agonist	8.92
5-HT_{2C}	6BQG	Active	Ergotamine	Agonist	11.19
5-HT_{2C}	6BQH	Inactive	Ritanserin	Inverse agonist	8.58

The analysis reveals a distribution of W6.48-ligand distances reflecting variability in ligand type, receptor state, and structural context. Nevertheless, inactive receptor states generally exhibit shorter W6.48-ligand distances than active conformations. Representative structures used for MD simulations were selected as well-resolved examples of both states, enabling a consistent comparison while acknowledging the limited structural sampling. Trends observed in MD simulations are consistent with those derived from crystallographic data. To compare the active and inactive states of the 5-HT_2 receptors, TRP-ligand distances were analysed using MD simulations based on experimentally determined structures (Figure 4). For the 5-HT_{2A}R receptor, W6.48-ligand distances were larger in the active G protein-coupled conformation {PDB ID: 7RAN, bound

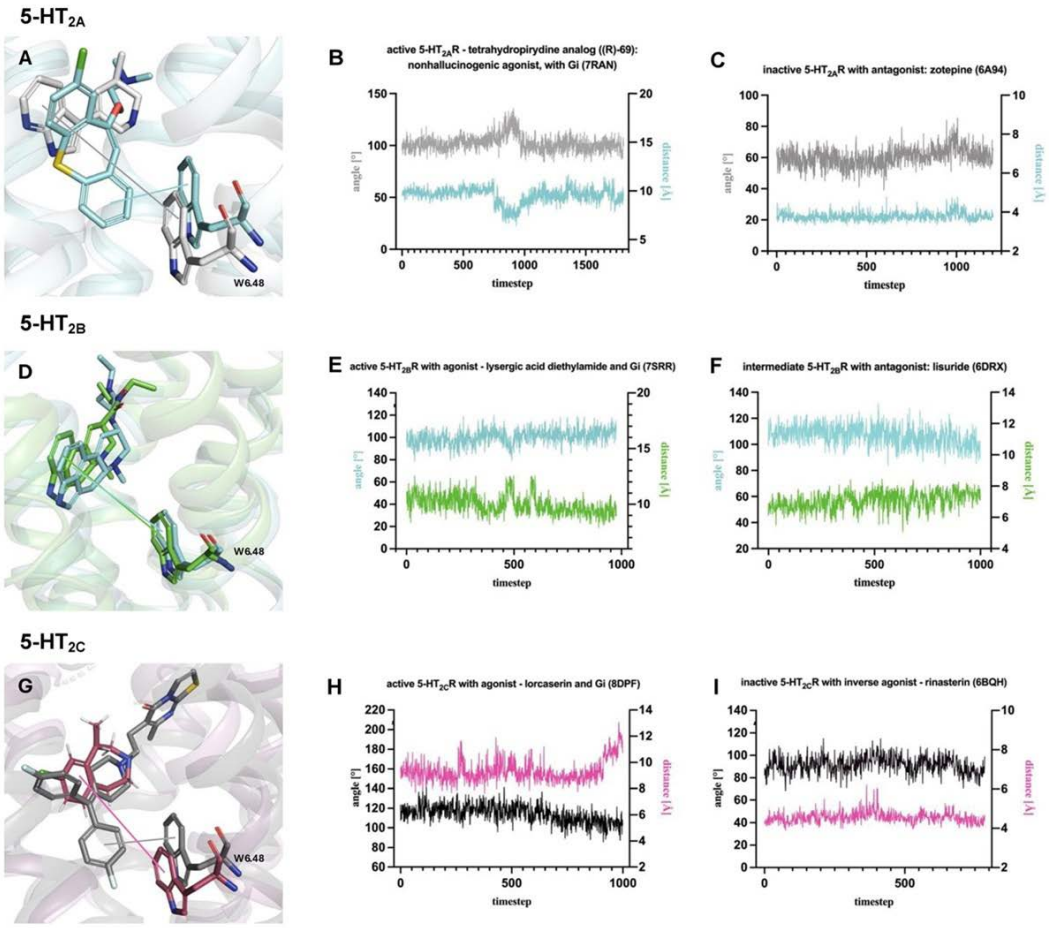

Figure 4. Aromatic interactions between ligands and W6.48 in 5-HT$_2$ receptors during molecular dynamics simulations (A, D, G); Representative binding poses of ligands in the orthosteric binding pockets of the 5-HT$_{2A}$R receptor, 5-HT$_{2B}$R receptor, and 5-HT$_{2C}$R receptor, highlighting W6.48. (B, C, E, F, H, I); Time evolution of the angle between the ligand aromatic ring and the indole ring of W6.48 (left axis) and the distance between the ring centres (right axis) during MD simulations of ligand-receptor complexes

to (3R)-3-methyl-5-(1H-pyrrolo[2,3-b]pyridin-3-yl)-1,2,3,6--tetrahydropyridin-1-ium (ligand ID: 3IQ), ~9 Å} than in the inactive structure bound to an antagonist [PDB ID: 6A94, bound to zotepine (ligand ID: ZOT), ~4 Å], indicating a more compact binding pocket in the inactive state. A comparable trend was observed for the 5-HT$_{2B}$R receptor. The active structure with agonist and G protein [PDB ID: 7SRR, bound to lysergic acid diethylamide (ligand ID: 7LD)] displayed expanded TRP-ligand separations (~9-11 Å), whereas the antagonist-bound intermediate structure [PDB ID: 6DRX, bound to lisuride (ligand ID: H8G)] showed shorter distances centred around ~6-7 Å. For the 5-HT$_{2C}$R receptor, TRP-ligand distances were similarly larger in the active G protein-coupled structure [PDB ID: 8DPF, bound to lorcaserin (ligand ID: T4U), ~8.5-10 Å] compared with the inactive antagonist-bound conformation [PDB ID: 6BQH, bound to ritanserin (ligand ID: E2J), ~4-5 Å], consistent with a compact inactive binding pocket. Analysis of TRP-ligand orientation revealed angles predominantly in the range of ~90°–120°, consistent with T-shaped aromatic interactions rather than parallel π–π stacking. In inactive receptors, shorter distances combined with this geometry suggest stabilising edge-to-face contacts between the ligand and W6.48. In the inactive 6A94 structure, angular values around ~60° suggest a tilted aromatic interaction between the ligand and W6.48. Conversely, upon receptor activation, increased TRP-ligand separation is observed, reflecting the displacement of W6.48 and expansion of the orthosteric binding pocket.

Conclusions

In this study, a large set of protein-ligand complexes was analysed to characterise the occurrence and interaction patterns of tryptophan residues in different protein classes. It was shown that tryptophan plays an important role in ligand binding and enzymatic functions, particularly among hydrolases, oxidoreductases, and transferases, as well as in proteins associated with the cell membrane and signalling. Gene Ontology analysis confirmed its importance in metal ion binding, protein-protein interactions, and redox-related biological processes. Geometric analysis of interactions between ligands and tryptophan revealed a clear preference for aromatic T-shaped configurations, i.e., perpendicular to the ligand rings, compared to classical π-π stacking, at distances consistent with stabilising aromatic interactions.

Within class A GPCRs, tryptophan-ligand interactions occurred in many receptor families. Molecular dynamics simulations of 5-HT_2 receptors reveal a consistent trend in which TRP-ligand distances vary across activation states. While these findings provide atomistic insights into the spatial relationships within the orthosteric pocket, they should be viewed as an illustrative comparison of representative states rather than a definitive mechanistic proof.

A limitation of this study is that the comparison between active and inactive receptor states is based on a single representative crystal structure for each receptor subtype. As a result, the observed differences in TRP–ligand distances may be influenced by structure-specific factors, including the nature of the co-crystallized ligand and experimental conditions. While the consistent trends observed across the analysed 5-HT_2 receptor subtypes suggest that these findings may reflect general structural tendencies, the limited structural sampling should be considered when interpreting the results. Future studies incorporating a broader set of experimentally determined structures could provide a more comprehensive and statistically robust characterization of these interactions.

In summary, these findings underscore the structural and dynamic roles of tryptophan in protein–ligand interactions, particularly within GPCR signalling. This work establishes a foundation for future structural investigations focused on ligand design and the development of compounds with defined pharmacological profiles.

Acknowledgments

The Authors gratefully acknowledge the Polish high-performance computing infrastructure PLGrid (HPC Center: ACK Cyfronet AGH) for providing computer facilities and support within the computational grant no. PLG/2025/019001.

References

[1] Bandyopadhyay A, Sarkar R. Site-selective cleavage of peptides and proteins targeting aromatic amino acid residues. RSC Advances. 2025;15(12):9159–9179. https://doi.org/10.1039/d4ra08956a.

[2] Barik S. The uniqueness of tryptophan in biology: Properties, metabolism, interactions and localization in proteins. International Journal of Molecular Sciences. 2020;21(22):8776. https://doi.org/10.3390/ijms21228776.

[3] Calinsky R, Levy Y. Aromatic residues in proteins: Re-evaluating the geometry and energetics of π-π, cation–π, and CH–π interactions. Journal of Physical Chemistry B. 2024;128(36):8687–8700. https://doi.org/10.1021/acs.jpcb.4c04774.

[4] Dougherty DA. The cation-π interaction. Accounts of Chemical Research. 2013;46(4):885-893. https://doi.org/10.1021/ar300265y.

[5] Szczygieł M, Derewenda U, Scheiner S, Minor W, Derewenda ZS. A structural role for tryptophan in proteins, and the ubiquitous TRP Cδ1-H···O=C (backbone) hydrogen bond. Acta Crystallographica Section D Structural Biology. 2024;80(Pt 7):551–562. https://doi.org/10.1107/S2059798324005515.

[6] Brylinski M. Aromatic interactions at the ligand-protein interface: Implications for the development of docking scoring functions. Chemical Biology and Drug Design. 2018;91(2):380–390. https://doi.org/10.1111/cbdd.13084.

[7] Shao J, Kuiper BP, Thunnissen AMWH, Cool RH, Zhou L, Huang C, Liu J, et al. The role of tryptophan in π interactions in proteins: An experimental approach. Journal of the American Chemical Society. 2022;144(30):13815––13822. https://doi.org/10.1021/jacs.2c04986.

[8] Lopez-Balastegui M, Stepniewski TM, Kogut-Günthel MM, Di Pizio A, Rosenkilde MM, Mao J, Selent J. Relevance of G protein-coupled receptor (GPCR) dynamics for receptor activation, signalling bias and allosteric modulation. British Journal of Pharmacology. 2025;182(14):3211–3224. https://doi.org/10.1111/bph.16495.

[9] Latorraca NR, Venkatakrishnan AJ, Dror RO. GPCR dynamics: Structures in motion. Chemical Reviews. 2017;117(1):139–155. https://doi.org/10.1021/acs.chemrev.6b00177.

[10] Trzaskowski B, Latek D, Yuan S, Ghoshdastider U, Debinski A, Filipek S. Action of molecular switches in GPCRs: Theoretical and experimental studies. Current Medicinal Chemistry. 2012;19(8):1090–1109. https://doi.org/10.2174/092986712799320556

[11] Plazinska A, Plazinski W, Luchowski R, Wnorowski A, Grudzinski W, Gruszecki WI. Ligand-induced action of the W286$^{6.48}$ rotamer toggle switch in the β_2-adrenergic receptor. Physical Chemistry Chemical Physics 2017;20(1):581–594. https://doi.org/10.1039/c7cp04808d.

[12] Nichols DE, Nichols CD. Serotonin receptors. Chemical Reviews. 2008;108(5):1614–1641. https://doi.org/10.1021/cr078224o.

[13] Voitel M, Pankonin M, Vogel A, Leitner K, Kaiser A, Huster D, Hildebran PW, Smith AA. Fine-tuning of the neuropeptide Y1 G protein-coupled receptor by the tryptophan$^{6.48}$ "Toggle Switch." Journal of the American Chemical Society. 2026;148(1):194–205. https://doi.org/10.1021/jacs.5c07143.

[14] Lee Y, Basith S, Choi S. Recent advances in structure-based drug design targeting class A G protein-coupled receptors utilizing crystal structures and computational simulations. Journal of Medicinal Chemistry. 2018;61(1):1–46. https://doi.org/10.1021/acs.jmedchem.6b01453.

[15] Kim J, Kim J, Choi C, Bae J, Choi HJ. Structural insights into GPCR signalling activated by peptide ligands: From molecular mechanism to therapeutic application. Experimental & Molecular Medicine. 2025;57(7):1467–1481. https://doi.org/10.1038/s12276-025-01497-y.

[16] Yuan S, Hu Z, Filipek S, Vogel H. W246$^{6.48}$ opens a gate for a continuous intrinsic water pathway during activation of the adenosine A_{2A} receptor. Angewandte Chemie: International Edition. 2015;54(2):556–559. https://doi.org/10.1002/anie.201409679.

[17] Peng Y, McCorvy JD, Harpsøe K, Lansu K, Yuan S, Popov P, Qu L, Pu M, Che T, Nikolajsen LF, Huang XP, Wu Y, Shen L, Bjørn-Yoshimoto WE, Ding K, Wacker D, Han GW, Cheng J, Katritch V, Jensen AA, Liu ZJ. 5-HT2C receptor structures reveal the structural basis of GPCR polypharmacology. Cell. 2018;72(4):719–730.e14. https://doi.org/10.1016/j.cell.2018.01.001.

[18] Yang J, Roy A, Zhang Y. BioLiP: A semi-manually curated database for biologically relevant ligand-protein interactions. Nucleic Acids Research. 2013;41:D1096-1103. https://doi.org/10.1093/nar/gks966.

[19] Zhang C, Zhang X, Freddolino PL, Zhang Y. BioLiP2: an updated structure database for biologically relevant ligand-protein interactions. Nucleic Acids Research. 2024.52(D1):D404–412. https://doi.org/10.1093/nar/gkad630.

[20] Lee J, Cheng X, Jo S, MacKerell AD, Klauda JB, Im W. CHARMM-GUI Input Generator for NAMD, Gromacs, Amber, Openmm, and CHARMM/OpenMM simulations using the CHARMM36 Additive Force Field. Biophysical Journal. 2016;110(3 suppl. 1):641a. https://doi.org/10.1016/j.bpj.2015.11.3431

[21] Kern NR, Lee J, Choi YK, Im W. CHARMM-GUI Multicomponent Assembler for modeling and simulation of complex multicomponent systems. Nature Communications. 2024;15(1):5459. https://doi.org/10.1038/s41467-024-49700-4.

[22] Lee J, Patel DS, Ståhle J, Park S-J, Kern NR, Kim S,Lee J, Cheng X, Valvano MV, Holst O, Knirel Y, Qi Y, Jo S, Klauda JB, Widmalm G, Im W. CHARMM-GUI Membrane Builder for complex biological membrane simulations with glycolipids and lipoglycans. Journal of Chemical Theory and Computation. 2019;15(1):775–786. https://doi.org/10.1021/acs.jctc.8b01066.

[23] Pytliak M, Vargová V, Mechírová V, Felšöci M. Serotonin receptors—from molecular biology to clinical applications. Physiological Research. 2011;60(1):15–25. https://doi.org/10.33549/physiolres.931903.

[24] Manglik A, Kruse AC. Structural basis for G protein-coupled receptor activation. Biochemistry. 2017;56(42):5628––5634. https://doi.org/10.1021/acs.biochem.7b00747.

[25] Weis WI, Kobilka BK. The molecular basis of G protein-coupled receptor activation. Annual Review of Biochemistry. 2018;87:897–919. https://doi.org/10.1146/annurev-biochem-060614-033910.

[26] Pándy-Szekeres G, Munk C, Tsonkov TM, Mordalski S, Harpsøe K, Hauser AS, Bojarski AJ, Gloriam DE. GPCRdb in 2018: Adding GPCR structure models and ligands. Nucleic Acids Research. 2018;46(D1):D440–446. https://doi.org/10.1093/nar/gkx1109.